ELSEVIER

Thermochimica Acta 269/270 (1995) 351–359

thermochimica acta

Solid state co-crystallization of sugar alcohols measured with differential scanning calorimetry☆

P. Perkkalainen *, H. Halttunen, I. Pitkänen

University of Jyväskylä, Department of Chemistry, P.O. Box 35 SF-40351 Jyväskylä, Finland

Received 16 September 1995; accepted 25 May 1995

Abstract

Mixtures of sugar alcohols xylitol, D-sorbitol and D-mannitol were prepared by grinding the solid starting materials together for 20 min. Possible co-crystals were identified by DSC and X-ray powder diffraction. The phase diagrams for the systems xylitol–D-sorbitol, xylitol–D-mannitol and D-sorbitol–D-mannitol were created using the peak values from the DSC measurements as melting points.

The phase diagram for xylitol and D-sorbitol showed that co-crystallization between these two components may be achieved by grinding them together. The powder diffraction pattern for a mixture of 0.50 mole fraction of xylitol and 0.50 mole fraction of D-sorbitol showed that the product consisted of both starting reagents and a new co-crystallization product. The melting point of the co-crystallization product was 75–77°C measured from the peak value of DSC measurements.

Keywords: Co-crystallization; DSC; D-Mannitol; Phase diagram; Sugar alcohols; D-Sorbitol; TG; X-ray powder diffraction; D-xylitol

1. Introduction

Binary systems can be divided according to their phase diagrams into eutectic systems, monotectic systems, systems forming solid solutions and systems forming solid complexes, i.e. co-crystals [1]. Hydrogen-bonded co-crystals can be prepared by solution co-crystallization, co-crystallization by sublimation or solid-state co-crystalli-

* Corresponding author. Fax: 358-41-602501.

☆ Presented at the 6th European Symposium on Thermal Analysis and Calorimetry, Grado, Italy, 11–16 September 1994.

SSDI 0040-6031(95)02539-1

zation [2]. The process of crystal growth in co-crystals follows the scheme:

Molecules ⇄ Aggregates ⇄ Crystals

Co-crystalline sugar alcohols are reported to be formed between xylitol and sorbitol [3] and sorbitol and mannitol [4]. Co-crystallized products are expected to have better tabletting and processing quality, and the melted co-crystals of xylitol containing sorbitol are reported to be less hygroscopic [3].

Xylitol, D-sorbitol (D-glucitol) and D-mannitol all exist in their most stable crystalline forms in the space group $P2_12_12_1$ [5–8]. D-Sorbitol and D-mannitol exist in several polymorphic forms [7–11]. Sugar alcohols are used as sweeteners in dietary and pharmaceutical products and as coatings in pharamaceutical tablets [3].

The aim of this study was to examine possible hydrogen-bonded co-crystals of monosaccaride alcohols formed by solid state co-crystallization and to create reference material for analysis of sugar alcohol mixtures. The effect of grinding on solid sugar alcohols was also examined.

2. Experimental

Mixtures of sugar alcohols xylitol–D-sorbitol, xylitol–D-mannitol and D-mannitol–D-sorbitol were prepared by weighing the reagents according to certain mole fractions. The reagents were D-sorbitol from Fluka, art. 85532 (purity > 98%, HPLC), D-(−)mannitol from Merck, art. 5982 (microbiological grade). The xylitol used was obtained from Cultor Ltd. and its purity was 99.9% (determined by Cultor Ltd.) The phases of the reagents and their thermal behaviour before and after grinding were confirmed with DSC and X-ray powder diffraction measurements. The D-(−)mannitol from Merck was monoclinic δ-form [10], the D-sorbitol from Fluka was a mixture of α- and Γ-polymorphs [8].

The mixtures were ground in a mill for 20 min. TG, DSC and X-ray powder diffraction measurements were carried out for each sample. The effect of grinding time was also examined. TG and DSC were used in the following hardware configurations (PE = Perkin-Elmer, HP = Hewlett-Packard):

TG: PE TGA7, TAC7/DX, IBM PS/2 Model 55SX, HP Plotter 7475A,
PE TADS.TGS(software)

DSC: PE DSC-7, TAC7/PC, EPSON PC AX2, HP Plotter 7475A,
PE DSC7(software).

The TG measurements were done in Pt pans in a current of air with a flow rate of 40–60 $cm^3\ min^{-1}$. The sample weights were 3–9 mg, the heating rate was 2°C min^{-1} and the temperature range 25–200°C. The DSC measurements were done in 50 µl aluminium pans with holes, in a current of nitrogen with a flow rate of 50–60 $cm^3\ min^{-1}$. The sample weights were 3–9 mg, the heating rate was 2°C min^{-1} and the temperature range varied from 25–120°C or from 25–180°C depending on the sample.

The X-ray powder diffraction patterns were measured with an ENRAF NONIUS PDS120 diffractometer equipped with an INEL CPS120 curved-position-sensitive detector, which allows simultaneous data recording of a diffraction pattern over a range of 120° of 2-theta. The radiation used was monochromatic $CuK\alpha_1$-radiation ($\lambda = 1.54056$ Å). Silicon powder (NBS 640b) was used as internal standard. The amount of internal standard added to the samples was 5 wt%.

3. Results and discussion

According to the TG measurements the samples did not contain significant amounts of moisture. The onset and peak temperatures of melting and the heats of fusion for the pure starting materials as well as for the pure starting materials ground in a grinding mill were determined by DSC. The mean values of two measurements and their derivations from the average are given in Table 1. The polymorphic forms of the starting materials were determined by DSC and by X-ray powder diffraction.

The phase diagrams for the systems xylitol–D-mannitol, D-mannitol–D-sorbitol and xylitol–D-sorbitol were constructed using the peak values for melting in the DSC curves, and are shown in Figs. 1–3. The use of resolidified melts for creating phase diagrams was unacceptable because of the possibility of polymorphic changes, and because the melts did not crystallize on cooling. The phase diagram for xylitol–D-sorbitol mixtures, which were ground separately, is shown in Fig. 4.

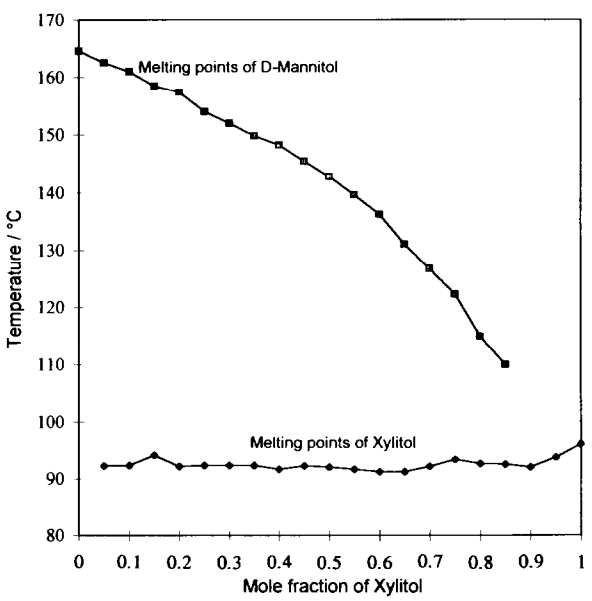

Fig. 1. The phase diagram for xylitol–D-mannitol.

Table 1
The mean values of the onsets and peaks of fusion and the heats of fusion for starting materials, measured by DSC. The deviation for the average are in parentheses.

Name and molecular formula	M/g mol^{-1}	Onset/°C	Peak/°C	ΔH/kJ mol^{-1}	Literature values				
					Onset/°C	Peak/°C	M.P./°C	ΔH/kJ mol^{-1}	Ref.
Xylitol $C_5H_{12}O_5$	152.1	93.0(0.5) (cryst.) 93.7(0.2) (ground)	94.3(0.6) (cryst.) 95.5(0.5) (ground)	36.4(0.3) (cryst.) 36.1(0.3) (ground)	90	100	93–94 92–94	38.0	[12] [5]
D-Sorbitol $C_6H_{14}O_6$	182.2	97.0(0.1) (cryst.) 96.8(0.1) (ground)	98.6(0.1) (cryst.) 98.7(0.2) (ground)	31.1(0.3) (cryst.) 30.2(0.5) (ground)			85(α-phase) 92(Γ-phase)		[6] [6]
D-Mannitol $C_6H_{14}O_6$	182.2	164.4(1.0) (cryst.) 162.7(0.6) (ground)	166.2(0.9) (cryst.) 165.2(0.6) (ground)	49.8(1.0) (cryst.) 49.2(0.1) (ground)	165.4	167.1	(δ-phase)	50.8	[10]

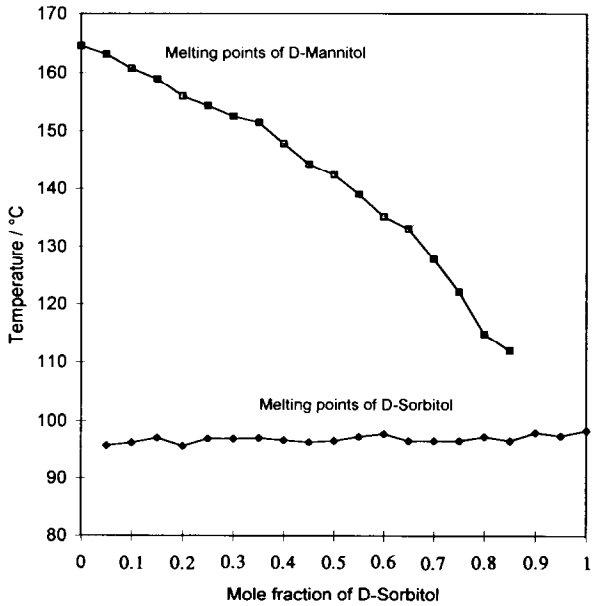

Fig. 2. The phase diagram for D-mannitol–D-sorbitol.

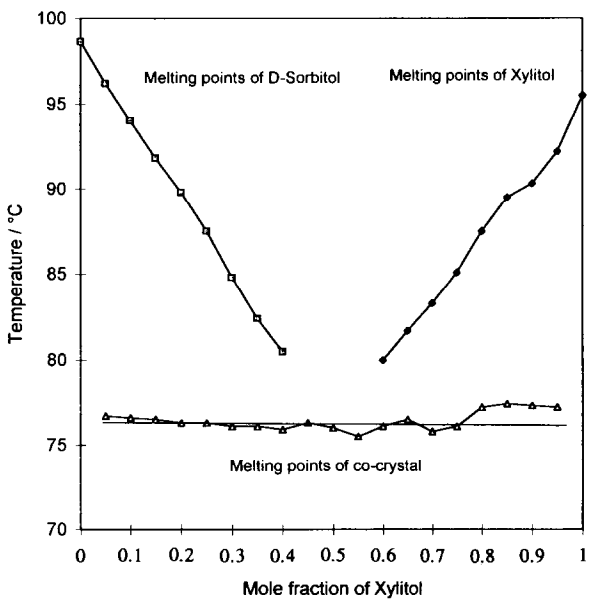

Fig. 3. The phase diagram for xylitol–D-sorbitol. The horizontal line is the mean value of the melting points of the co-crystal between the xylitol/D-sorbitol mole fractions 0.25/0.75 and 0.75/0.25.

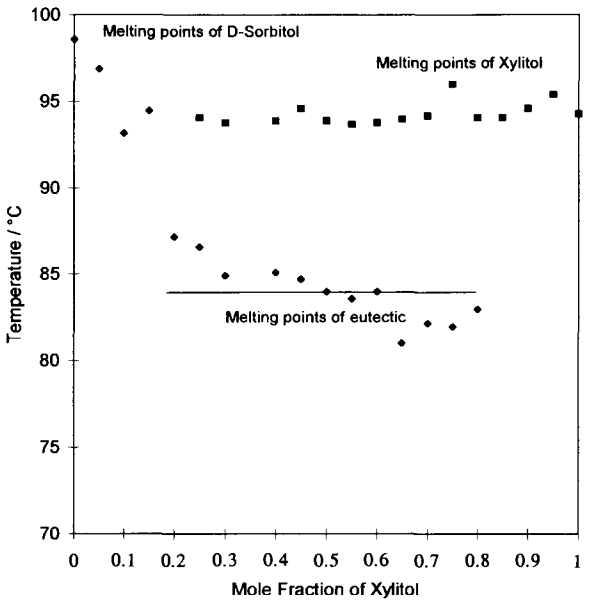

Fig. 4. The phase diagram for mixtures of xylitol and D-sorbitol ground separately. The horizontal line is the mean value of the melting points of eutectic between the xylitol/D-sorbitol mole fractions 0.20/0.80 and 0.80/0.20.

The phase diagrams for the mixtures of xylitol–D-mannitol and D-sorbitol–D-mannitol were monotectic. The melting point of the sugar alcohol with a lower melting point (xylitol or D-sorbitol) was only slightly affected by the presence of the substance with a higher melting point (D-mannitol). The mean values and the standard deviations (in parentheses) for the peak values of the fusion of xylitol and D-sorbitol in these mixtures were 92.3 (0.7)°C and 96.6 (0.6)°C, respectively, and the enthalpies of fusion were 36.6 (1.6) kJ mol^{-1} and 34.4 (1.9) kJ mol^{-1}, respectively, when calculated between the mole fractions of 0.05/0.95 and 0.95/0.05 of xylitol or D-sorbitol/D-mannitol. The melting peak values and the heats of fusion were slightly different from the values obtained for the pure starting materials (Table 1). These changes can be due to errors in the crystal lattice when a small amount of a foreign sugar alcohol has entered the lattice of the host sugar alcohol thus forming a substitutional solid solution.

The melting point of D-mannitol was lowered as the mole fraction of xylitol or D-sorbitol increased. This was due to the solubility of D-mannitol in melted xylitol or in melted D-sorbitol. When the component with a lower melting point had melted, the system contained melted xylitol (or sorbitol) with D-mannitol both in solution and in the crystalline form. The measured values for the total heats of the melting processes of these samples were in line with the values calculated from the heats of fusion of the pure samples when their mole fraction was taken into account. The shapes of the DSC curves for the samples, which were made by grinding the starting materials separately and

mixing them, were similar to the DSC curves obtained for the samples made by grinding the starting materials together.

The phase diagram for xylitol–D-sorbitol differed from those of the other two systems. It followed the usual form of eutectic phase diagram, but the phase diagram obtained for the samples ground separately and mixed together (Fig. 4.) differed from the phase diagram obtained for the samples, which were ground together (Fig. 3.). The phase diagram for xylitol–D-sorbitol samples, which were ground separately, was monotectic. The melting points of xylitol were not affected by the presence of D-sorbitol, but the melting point of D-sorbitol was lowered as the mole fraction of xylitol was increased. Because the peak values of the lower endotherms in the mole fraction area of 0.20/0.80–0.80/0.20 of xylitol/D-sorbitol were quite stable, was this referred to as eutectic melting. The mean value and the standard deviation of the mean for the eutecic melting peak in the molefraction area of 0.20/0.80–0.80/0.20 of xylitol–D-sorbitol were 84.0(1.8)°C.

The DSC figures for the samples made by grinding the starting material together did not have the shape of eutectic melting, which would have been observed as a sharp melting peak in the DSC curve [13]. The DSC curves of the samples, which were ground separately and mixed together, differed from the DSC curves of the samples ground together (Fig. 5). Eutectic melting could be detected as an inversion point in the DSC curves of the samples made by grinding the starting materials together.

In the phase diagram of xylitol–D-sorbitol (Fig. 3) the intersection of the two lines gives 76.2°C as the melting point and 0.495/0.505 (xylitol/D-sorbitol) as the mole fraction of the co-crystal. The mean value and the standard deviation for the peak

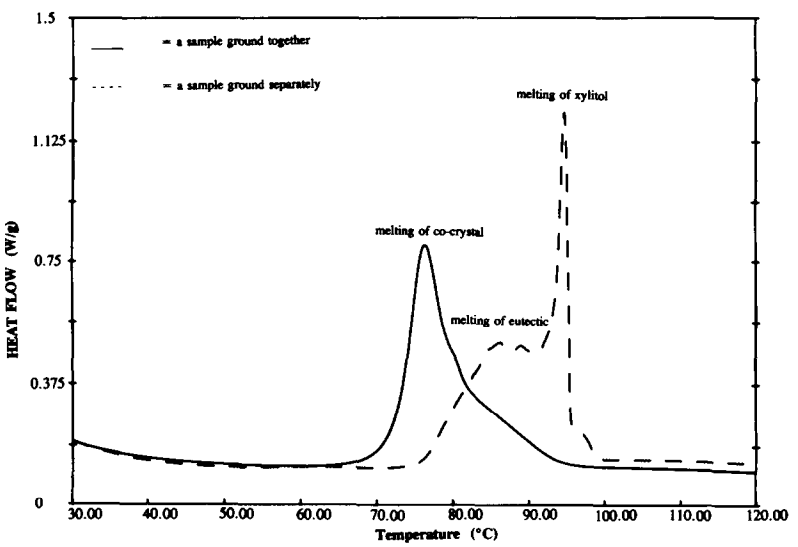

Fig. 5. The normalized DSC curves of the samples of xylitol and D-sorbitol ground together and ground separately.

values of melting calculated between mole fractions 0.25/0.75 and 0.75/0.25 was 76.1 (0.3)°C. In the area of mole fraction 0.8/0.2–0.95/0.05 of xylitol/D-sorbitol a slight drop can be observed in the Fig. 3. In the same mole fraction area, the melting point of the co-crystal changes also. It is possible that another co-crystal is formed in this mole fraction area.

It is obvious that the samples made by grinding xylitol and D-sorbitol together in a mill for 20 min also contained co-crystalline material. The X-ray powder diffraction measurements confirmed that these samples contained, in addition to the pure starting materials, some new product whose appearance could be observed by an extra peak arising in the powder diffraction pattern in Fig. 6.

The effect of the grinding time was examined with a sample containing 0.50 mole fraction of xylitol and 0.50 mole fraction of D-sorbitol. The grinding time did not affect the values of melting peaks or onsets, but the whole enthalpy of fusion was decreased with increasing grinding time; with 20 min grinding time the whole enthalpy of fusion was 29.8 kJ mol^{-1} and with 60 min grinding time, 27.7 kJ mol^{-1}. An interesting observation was that the shape of the melting peak of the co-crystal in the DSC curves became sharper as the grinding time was increased, thus indicating the formation of co-crystalline material.

One can assume that the reason for co-crystals being formed in xylitol–D-sorbitol systems, but not in the other two systems, is that the energy brought to the system by grinding is large enough to cause melting in the microcrystalline areas of these starting materials. As the melting points and heats of fusion of xylitol and D-sorbitol are very similar, both sugar alcohols are nearly equally affected by the increase in energy, and the melting in the microcrystalline areas of both sugar alcohols takes place almost simultaneously. In addition, both sugar alcohols exist in their crystal structure in the

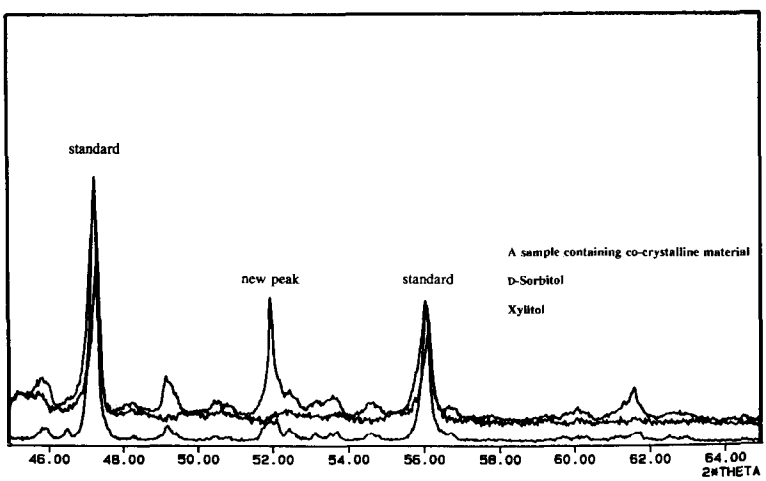

Fig. 6. The X-ray powder diffraction patterns of xylitol, D-sorbitol and a sample containing co-crystalline material.

space group $P2_12_12_1$, and both xylitol and D-sorbitol have very similar conformations in their carbon skeleton, D-sorbitol being only CH_2OH unit larger than xylitol. Although the phase diagrams for the mixtures of xylitol–D-mannitol and D-sorbitol–D-mannitol did not show signs of co-crystallization in the solid state, it may be possible to get co-crystals by melting them together [3, 4]. Our next interest is to prepare melted co-crystals from these sugar alcohols.

References

[1] J.L. Ford and P. Timmins, Pharmaceutical Thermal Analysis, Techniques and Applications, Ellis Horwood, Southampton, 1989, Chapter 2.
[2] G.M. Frankenbach, The Preparation and Characterization of Hydrogen-bonded Co-crystals with Applications to Materials Science, Ph.D. Thesis, University of Minnesota, June 1989, Chapter 1.
[3] J.W. DuRoss, U.S. Patent 5158789 A.
[4] J.W. DuRoss, Eur. Patent 347121 A2(A3).
[5] H.S. Kim and G.A. Jeffrey, Acta Crystallogr. Sect. B: 25 (1969) 2607.
[6] Y.J. Park, G.A. Jeffrey and W.C. Hamilton, Acta Crystallogr. Sect. B:, 27 (1971) 2393.
[7] H.M. Berman, G.A. Jeffrey and R.D. Rosenstein, Acta Crystallogr. Sect. B:, 24 (1968) 442.
[8] H.S. Kim, G.A. Jeffrey and R.D. Rosenstein, Acta Crystallogr. Sect. B:, 24 (1968) 1449.
[9] S. Quinquenet, M. Ollivon, C. Grabielle-Madelmont and M. Serpelloni, Thermochim. Acta, 125 (1988) 125.
[10] I. Pitakänen, P. Perkkalainen and H. Rautiainen, Thermochim. Acta, 214 (1993) 157.
[11] F.T. Jones and K.S. Lee, Microscope, 18 (1970) 279.
[12] A. Reamy and F. Schweizer, J. Therm. Anal., 28 (1983) 95.
[13] J. Sestak, Thermophysical properties of solids; their measurements and theoretical thermal analysis in G. Svehla (Ed.), Comprehensive Analytical Chemistry, Volume XII Thermal Analysis, Part D, Wilson and Wilson, 1984, pp 325–328.